EMITTANCE MEASUREMENTS AT THE NEW UNILAC PRE-STRIPPER USING A PEPPER-POT WITH A PC-CONTROLLED CCD-CAMERA

M. Dolinska[1], M. Domke, P. Forck, T. Hoffmann, D. Liakin[2], A. Peters, P. Strehl

GSI, Darmstadt, Germany.

Abstract:

The complex mathematical algorithms and procedures to extract emittance data from intensity distributions measured with a single shot pepper-pot device are described. First results of mathematical evaluation from the commissioning of the new GSI pre-stripper linac structures are presented.

1 INTRODUCTION

At present commissioning of the new UNILAC pre-stripper is performed. To assess the performance of new types of ion sources, fluctuations of beam emittances from pulse to pulse and, even within one pulse, a single shot pepper-pot system has been developed. The design criteria have been already reported in [1].

2 STRUCTURE OF SOFTWARE

The software was designed to provide the interconnection between all parts of the installed measuring hardware, a user friendly interface for hardware control and a detailed graphical output for the obtained results. Figure 1 shows the general structure of the software. To control the CCD camera the manufacturer developed system drivers and DLL's have been used. This offers the operator the possibility to change the operation mode of the camera, the exposure time, the resolution and some other parameters related to the actual parameters of the ion beam or the calibration signal. Furthermore, in case of low intensity of the observed light spots it is possible to integrate a series of single shots to improve the quality of the images.

The objective of the CCD-camera is controlled by means of the Tiger-BASIC based microprocessor system, which has been connected to the PC through a conventional RS485 interface. Therefore, no additional system driver had to be installed.

The collected data may be processed immediately via the "Calculation routines DLL" for evaluation of emittances or may be stored on the hard disk in binary or ASCII format for later calculations. Additionally, data may be saved and reloaded in Windows bitmap format.

Information about a current measurement, including commentary and preview pictures, are stored in the local database to provide easiest and systematic access to all
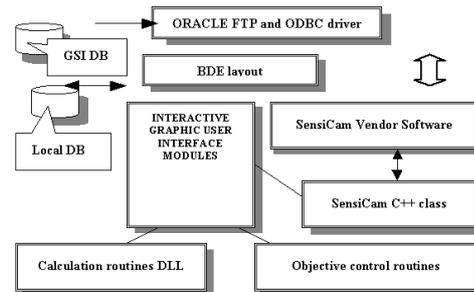
Figure 1: General structure of the pepper-pot system software

results. Information about the kind of accelerated ions, their charges, energy etc., is obtained from the global GSI database.

3 DATA PROCESSING

3.1 Calibration procedure

In the calibration process a parallel light beam from a laser (see [1] for details) is used to determine the correspondence between the pixels of the camera image and the real physical dimensions. It is assumed that the coordinates on the image, correlated to the locations of the holes in the pepper-pot plate can be obtained from the center of intensity of each light spot. Since all spots of the pepper-pot holes are arranged in the nodes of a regular rectangle grid it is sufficient to apply the implemented searching algorithm only for a whole row or column. The results are stored as reference information for future calculations in the project database.
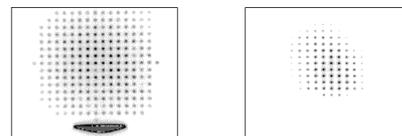
Figure 2: Light spots from the calibration with the laser beam (left) and real beam data, obtained with the CCD – camera.

---

[1] INR-Kiev, work done at GSI

[2] ITEP-Moscow, work done at GSI

3.2 A practical, fully implemented algorithm for determination of emittances

The set of light spots on the viewing screen, having different brightness levels, shapes and sizes represents the intensity distribution in the 4-dimensional phase space. Obviously, if the emittances of the two transverse phase planes can be considered to be independent of each other the same information about the intensity
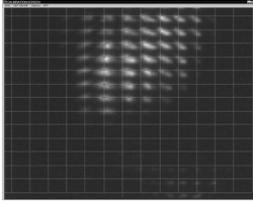
Figure 3: Spots of a Ni-beam on the viewing screen behind the pepper-pot.

distribution in the 2-dimensional phase planes should be contained within each row considering the horizontal phase plane, respectively within each column (vertical phase plane). Therefore, a simplified algorithm for emittance calculations based on the conventional slit-detector measurement ideology has been implemented
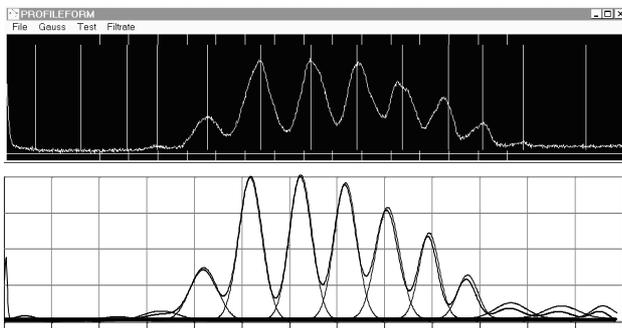
Figure 4: Non-linear grid manually adjusted in the PROFILE window(top) fitted curve (bottom).

and will be explained considering the measured spot pattern of Fig. 3. Due to the finite emittance of the ion beam no regular grid can be fitted to this light spot pattern. An interactive graphic tool has been implemented to give a skilled operator the possibility to generate a nonlinear grid as shown for example in Fig. 4.
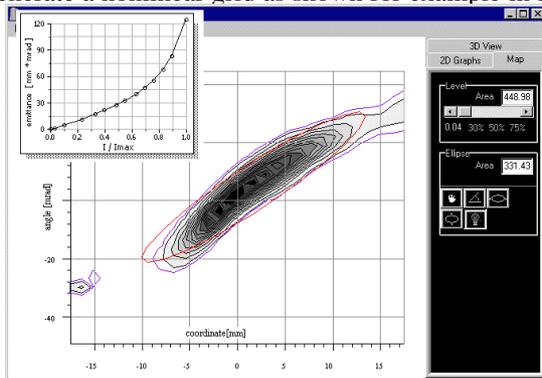
Figure 5: Horizontal emittance contour map window and emittance-current dependence (top left corner).

Here the ticks on top of the figure represent the observed light spot position from the calibration procedure. The long lines have been adjusted manually by an operator. To improve the separation of the peaks a fit procedure assuming Gaussian shapes of the peaks can be applied to the data as also shown in Fig. 4. As a result we get the divergences along each row or column of the pepper-pot holes. Referring to the conventional slit-detector system this corresponds to the profile measurements behind the slit. To prepare the data for further processing a cubic 2D spline fit is applied to interpolate data between lines. For calculation of the relevant emittance parameters and to provide graphics output in kind of maps like Figure 5, trees of contours corresponding to different intensity levels are created. Additionally, the program gives possibility to display and to print 3D surfaces of processed data sets.

3.3 Description of a second, pure mathematical algorithm

For exploitation of the experimental results the recorded images are treated digitally by a numerical data analysis program. The main procedures of the image
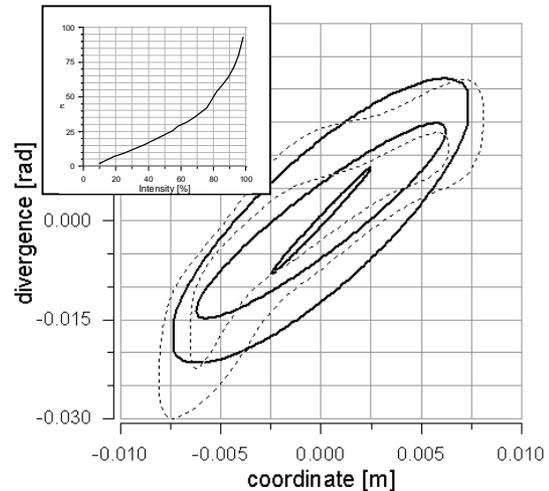
Figure 6: The lines of equal intensity and their best fitted ellipses built by the new algorithm (see text).

processing algorithms can be characterised as follows:

- In a first step a smoothing process along all pixels in each line of the image is performed. It has been decided to use the least squares method with Legendre polynomials as a basis. The discrete function I=I(x) is approximated in the interval $[x_0, x_n]$ by polynomials:

$$I(x) = \sum_{k=0}^{m} c_k \cdot L_k(x),$$

with $m \leq n$. Figure 7 demonstrates the effect of smoothing. Experience has shown that it is sufficient to apply the smoothing procedure only along the horizontal pixel-lines. After the smoothing
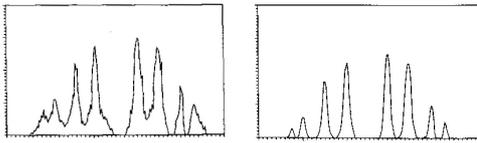
Figure 7: Measured data along one pixel line(left) and after smoothing(right)

procedure has been carried out the information about the intensity distribution $I(i,j)$ is available. Here i,j are the numbers of a pixel ($i=1…1280$, $j=1…1024$).

- Next is a procedure to detect and distinguish each spot. The algorithm starts at the position of the centre hole defined by the laser calibration. Two cases have to be considered: in the simple case the spot is placed around a hole and therefore the position of the spot is known. In the second case the spot is placed in some distance from the hole which means the intensity at the hole is zero. In this case a spot searching routine will be applied looking in a spiral motion pixel by pixel around the hole position. Assuming no overlap due to very large emittances, all detected spots can be definitively assigned to a hole. Figure 8 gives an example of one detected spot.
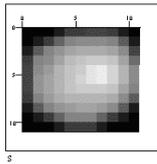
Figure 8: Example of a detected spot

- In the third step the vertical and horizontal size of each spot is determined. The routine starts at the detected spot, looking for the borders in the 4 coordinate directions (x, -x, y, -y) characterising the spot sizes in 4 directions: left, right, up and down.

- For further processing the two projections (vertical and horizontal) of one spot are needed. Determining the maximum values along all vertical lines the horizontal projected peak will be found. Applying the same procedure along all horizontal lines the vertical projected peak can be found.

- Next step is an approximation of the projected spot curves by Gaussian functions. Since in general the projections will not be of symmetrical shape, the left
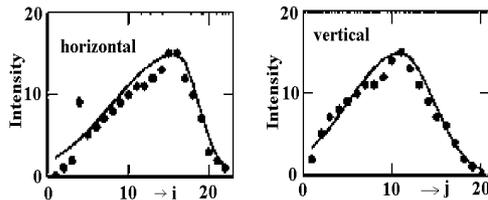
Figure 9: Projected peaks and corresponding Gaussian approximation.

and right sides of the curves are described separately by two Gaussian functions. As a result, each spot is described by 4 Gaussian functions (2 for each direction) determined by σ_r, σ_l, σ_u, σ_d, the maximum intensity I_o, and Δx, Δy to describe the location in relation to the corresponding hole position. Figure 9 shows two projected peaks from experimental data and the approximation by the 4 Gaussian functions. Using the Gaussian approximations it is now possible to determine the divergences for different fractions of the maximum intensity. From the formula

$$I(x) = I_0 \cdot \exp(-\frac{(x-x_0)^2}{2\sigma^2})$$

the linear deviation is determined by

$$\Delta x = \sigma \cdot \sqrt{2 \cdot \ln \frac{I_0}{I(x)}}.$$

First, the set of data has to be normalised to the maximum intensity. Then, as an example, the divergence XR' is given by

$$XR' = \frac{(dx + \Delta xr) \cdot h}{L}$$

with $dx = x_o - x_{hole}$, where x_o is the position of the maximum intensity within a spot and x_{hole} is the coordinate of the corresponding hole. The value of h is determined by $h = \Delta h/N_p$, where Δh is the spacing between two holes and N_p is the number of pixels between two holes. In terms of the fractions PR [$0 \leq PR \leq 1$] and the normalised intensity IN_m, Δxr is given by

$$\Delta xr = \sigma r \cdot \sqrt{2 \cdot \ln\left(\frac{IN_m}{PR}\right)}.$$

- In the next step 5 matrixes are formed. Four matrixes XR', XL',YU',YD' describing the divergence in the directions left, right, up, down and one matrix representing the total spot intensities. To determine now the 2-dimensional emittance in the horizontal phase plane the averages for each vertical column are calculated. Since the coordinate in x-direction is given by the index i of each column the phase plot is determined.

- For the determination of Twiss parameters a graphical method as well as the statistical evaluation can be applied.
 The results of the calculation shown in Fig. 6 agree with the results obtained earlier (see Fig. 5).

REFERENCES

[1] Domke, M. et al., DIPAC 1997, LNF-INFN Frascati, (1997), p. 141-143.